# Steel slag filter design criteria for phosphorus removal from wastewater in decentralized applications

By Dominique Claveau-Mallet[1], Étienne Boutet[2] and Yves Comeau[1]

[1]Department of Civil, Geological and Mining Engineering, Polytechnique Montreal, Montreal, Quebec, Canada, H3C 3A7

[2]Bionest, 55, 12[e] Rue, C.P. 10070, Shawinigan, Quebec, Canada, G9T 5K7

* corresponding author: dominique.claveau-mallet@polymtl.ca

## Abstract

The objective of this project was to develop a novel phosphorus removal system using steel slag filters applicable in decentralized applications and to propose design criteria about maintenance needs. Slag exhaustion functions were measured on 2-3 mm, 3-5 mm, 5-10 mm and 16-23 mm slag. Three steel slag columns with particle size of 2-3 mm, 3-5 mm and 5-10 mm were fed with the effluent of an aerated lagoon during 589 days. A barrel reactor test was fed during 365 days with the effluent of an attached growth aerated biological reactor. The o-$PO_4$ concentration at the effluent of the 2-3 mm and 3-5 mm columns and barrel reactor test was between 0.04 and 0.3 mg P/L. Particulate phosphorus, however, was removed by about 50%. The P-Hydroslag model implemented in PHREEQC was successfully calibrated with data from the column test, and validated with data from the barrel reactor test. The calibrated model was used to simulate long-term operation of a slag barrel reactor with two parallel streams of five replaceable steel slag barrels, with total hydraulic retention time of voids of 15 h. The system longevity was strongly influenced by the influent alkalinity. The simulated longevity was 7 years with an influent alkalinity of 50 mg $CaCO_3$/L and 2 years with an influent of 210 mg $CaCO_3$/L. The

alkalinity of the steel slag filter influent was influenced by the type of aquifer supplying drinking water, the presence of nitrification activity and by the $CO_2$ concentration in the enriched air of the upstream biological process. Simulated scenarios with partial barrel replacement (e. g. barrels 1 and 2 out of 5 replaced at frequency of 0.5, 1, 1.5, 2, 2.5, 3, 3.5 or 4 years) increased the system longevity up to 14 years while slightly increasing the number of barrels needed.

## Keywords

P-Hydroslag; physicochemical modeling; alkalinity; reactive filter; PHREEQC

## Abbreviations

| Symbol | Description | Formula or Units |
|---|---|---|
| **General abbreviations** | | |
| EAF | Electric arc furnace | |
| $HRT_V$ | Hydraulic retention time of voids | h |
| o-$PO_4$ | Orthophosphates | mg P/L |
| TIC | Total inorganic carbon | mg C/L |
| TP | Total phosphorus | mg P/L |
| TSS | Total suspended solids | mg/L |
| **Abbreviations for mineral phases** | | |
| CAL | Calcite | $CaCO_3$ |
| HAP | Hydroxyapatite | $Ca_5OH(PO_4)_3$ |
| MON | Monetite | $CaHPO_4$ |
| **Constants** | | |
| $a_{CaCl2}$ | Stochiometric coefficient of $CaCl_2$ in slag | [-] |

| | | |
|---|---|---|
| $a_{CaO}$ | Stochiometric coefficient of CaO in slag | [-] |
| $B_1$ and $B_2$ | Regression coefficients in $k_{diss}$ exhaustion function | |
| $D^*$ | Dispersivity (transport model) | [cm] |
| $D_{barr}$ | Diffusion coefficient in the crystal barrier | [$m^2/s$] |
| $D_n$ | Exchange factor between effective and immobile porosity (transport model) | [$s^{-1}$] |
| $k_{CAL}$ | CAL precipitation constant | [mol CAL/s $m^2$ slag] |
| $k_{HAP}$ | HAP precipitation constant | [mol HAP/s $m^2$ slag] |
| $k_{MON}$ | MON precipitation constant | [mol MON/s $m^2$ slag] |
| $n_e$ | Effective porosity in the slag filter | [-] |
| $P_1$, $P_2$, $P_3$ and $P_4$ | Regression coefficients in $pH_{sat}$ exhaustion function | |
| $S$ | Slag specific surface | [$m^2/m^3$] |

**Rates, functions and variables**

| | | |
|---|---|---|
| $CaOl_{TOT}$ | Cumulative leached CaO in a batch test | [mol/g] |
| $k_{diss}$ | Slag dissolution constant | [mol CaO/$m^2$ slag] |
| $pH_{sat}$ | Saturation pH in the slag filter | [-] |

# 1 Introduction

Phosphorus removal from wastewater in decentralized applications (influent flowrate below 3600 L/d) is a challenge because low costs and low maintenance associated with small-scale systems are not compatible with phosphorus-removal technologies used in large scale facilities (Brunce et al. 2018). Steel slag filters are attractive for domestic wastewater treatment in decentralized applications because of their high phosphorus removal efficiency, low costs and potential low maintenance needs (Zuo et al. 2017). Effluent o-$PO_4$ concentration as low as 0.1

mg P/L were observed in recent studies in which steel slag filters were fed with synthetic domestic wastewater (Blanco et al. 2016), real domestic wastewater (Hussain et al. 2015) or pretreated fish farm effluent (Kõiv et al. 2016). Steel slag filters were also used in lab-scale studies for the treatment of wastewater with high o-$PO_4$ concentration (90 mg P/L, Park et al. 2017) or low o-$PO_4$ concentration (0.025-0.03 mg P/L, Postila et al. 2017). Yet, steel slag filters are not commonly used for domestic wastewater treatment in decentralized applications because of the need for neutralizing the alkaline effluent and handling the media replacement at a reasonable cost.

The main issue related to steel slag filters is the sudden drop in phosphorus removal efficiency following slag exhaustion (Park et al. 2017). Slag exhaustion involves slag replacement which requires longevity prediction and a design tool. Some research teams have attempted to develop longevity prediction tools based on empirical relationship using the slag CaO content and its retention capacity (Vohla et al. 2011) or using slag properties, hydraulic retention time and phosphorus concentration (Penn et al. 2016). Recently, the P-Hydroslag model was developed for the prediction of steel slag filter longevity (Claveau-Mallet et al. 2017). This mechanistic model was calibrated with synthetic wastewater and could predict breakthrough curves of pH, o-$PO_4$, calcium and alkalinity of steel slag filters. A preliminary version of the model was used for design applications (Claveau-Mallet et al. 2015, Kõiv et al. 2016), but this model remains to be formally validated.

In past studies, limited attention was given to particulate phosphorus in steel slag filters. The focus was on o-$PO_4$ removal. The fate of particulate phosphorus from influent suspended solids or from newly formed calcium-phosphates was not specifically addressed. In full-scale applications, the fate of both soluble and particulate phosphorus should be understood,

because tertiary treatment regulations are based on total phosphorus (Metcalf and Eddy - AECOM 2014).

The objective of this project was to develop a novel phosphorus removal system using steel slag filters applicable in decentralized applications and to propose design criteria about maintenance needs.

# 2 Materials and Methods

## 2.1 Slag media

The slag media (electric arc furnace steel slag) was produced by Arcelor Mittal and provided by Minéraux Harsco (Contrecoeur, Canada). The slag properties are presented in Table 1 and were determined in a previous study (Claveau-Mallet et al. 2017).

*Table 1: Electric arc furnace steel slag properties*

| Property | Units | Value |
|---|---|---|
| Density* | g/mL | 3.8 |
| Specific surface* | $m^2/g$ | 0.308 |
| Chemical composition* | % | $Fe_2O_3$: 33; CaO: 30; $SiO_2$: 16; MgO: 12; $Al_2O_3$: 6; others oxides: 3 |
| Grain size | - | 16-23 mm; 5-10 mm; 3-5 mm; 2-3 mm |

*measured on a 5-10 mm sample by Claveau-Mallet et al. (2017)

## 2.2 Determination of exhaustion functions

The principle behind exhaustion functions is to measure the reactive potential of a slag sample in successive batch tests. In each batch test, the saturation pH and dissolution kinetic constant were determined by numerical inversion. Between batch tests, the slag sample was aged with acid baths using $HNO_3$ 0.0625 M, which resulted in decreasing the saturation pH and dissolution

kinetic constant. The exhaustion functions were obtained by regression from plots of slag dissolution parameters (saturation pH and dissolution kinetic constant) against total leached CaO. The full description of the experimental methods and construction procedure of the exhaustion functions is provided in Claveau-Mallet et al. (2017).

Three exhaustion functions were measured on three 300-g slag samples with particle size of 2-3 mm, 3-5 mm and 16-23 mm. Slag was sieved in the laboratory. Batch tests were conducted with 700 mL of synthetic wastewater composed of tap water and lab-grade salts ($KH_2PO_4$, $K_2HPO_4$, $CaCl_2{\cdot}2H_2O$ and $NaHCO_3$). The synthetic wastewater composition was pH 7.7 ± 0.2, o-$PO_4$ 9.3 ± 0.2 mg P/L, Ca 46 ± 2 mg/L and total inorganic carbon (TIC) 22.6 ± 0.5 mg/L. The batch test water was analyzed at the beginning and the end of the test for pH, o-$PO_4$, filtered TIC and filtered calcium. In the numerical inversion, precipitation constants were fixed at $k_{HAP} = 10^{-11.03}$ mol $s^{-1}$ $m^{-2}$, $k_{MON} = 10^{-8.67}$ mol $s^{-1}$ $m^{-2}$ and $k_{CAL} = 10^{-9}$ mol $s^{-1}$ $m^{-2}$ (Claveau-Mallet et al. 2017).

## 2.3 The Grandes-Piles WRRF

Both column tests and the barrel reactor tests were conducted at the Grandes-Piles (Quebec, Canada) Water Resource Recovery Facility (WRRF). The Grandes-Piles WRRF consists of two vertical walls aerated lagoons where a KAMAK process (Bionest Wastewater Treatment Solutions 2018) is installed in the upstream two-third of the first lagoon. The KAMAK system is a lagoon treatment enhancement technology where three settling and clarification zones are separated by two aerated fixed media biofilm reactors. The Grandes-Piles WRRF influent flowrate is 130 $m^3$/d (2013 data). The WRRF effluent data was divided into two periods for the calculation of mean values (Table 2). The two periods did not have the same alkalinity at the WRRF effluent because of changes in bicarbonate addition to the lagoons and variations in the process nitrification efficiency.

The column tests were conducted with the WRRF effluent.

*Table 2 Composition of the Grandes-Piles WRRF and attached growth aerated reactor effluents*

| Parameter | Units | WRRF effluent t = 0 to 100 d | WRRF effluent t = 100 to 589 d | Attached growth reactor effluent |
|---|---|---|---|---|
| pH | - | 7.64 | 7.26 | 7.67 |
| Alk | mg $CaCO_3$/L | 192 | 86 | 61 |
| TP | mg P/L | 5.1 | 5.1 | 5.1 |
| o-$PO_4$ | mg P/L | 4.6 | 3.5 | 5.0 |
| Dissolved Ca | mg/L | 15 | 15 | 28 |
| TSS | mg/L | 17 | 20 | 15 |
| $CBOD_5$ | mg/L | 22 | 18 | 15 |
| Effluent used as influent of : | | column tests | | barrel reactor test |

The barrel reactor test were conducted using a full-scale on-site treatment system for a 3-bedroom-house which consisted of a septic tank followed by an attached growth aerated reactor. The Grandes-Piles influent was used to feed the septic tank in batch mode (6 h - 9 h; 11 h - 14 h and 17 h - 20 h). The attached growth aerated reactor was fed by the septic tank. The main composition of the slag filter tests influent is presented in Table 2 and in Appendix.

## 2.4 Column tests

The column tests were used for model calibration. Three slag filter columns (length = 79 cm and diameter = 15.1 cm) were fed with the effluent of the WRRF during 589 d (May 2016 to Dec 2017) in a continuous flow mode (Table 3). The 2-3 mm and 3-5 mm slags were sieved at Grandes-Piles from a 0-5 mm bulk batch. The porosity was determined at the beginning of the test from filling and emptying the filters with water. At the time of filling, the column was allowed to rest 2 hours. The needed water volume to completely fill the column was measured and this volume was assumed to correspond to the void volume of the filter. The filling-emptying procedure was repeated until the needed volume was constant (three times, volumes

presented in Table 3). The column influent and effluent was sampled once a week and analyzed for pH, o-$PO_4$, TP, alkalinity and calcium.

*Table 3: Column tests set-up*

| Column | Grain size | Void volume (L) | | | Porosity | $HRT_V$ |
|---|---|---|---|---|---|---|
| - | mm | 1st fill | 2nd fill | 3rd fill | % | h |
| 1 | 2-3 | 6.9 | 6.0 | 6.1 | 40 | 16 |
| 2 | 3-5 | 6.8 | 6.1 | 6.1 | 40 | 16 |
| 3 | 5-10 | 6.9 | 6.3 | 6.3 | 40 | 16 |

## 2.5 Barrel reactor test

The barrel reactor test was conducted from February 2017 to February 2018 at the Grandes-Piles WRRF and was used for model validation. The barrel reactor was a novel wastewater treatment system composed of an underground concrete reactor containing ten slag barrels (Boutet et al. 2017). The attached growth reactor effluent was sent to the barrel reactor and was divided into two parallel five-barrel streams according to the batch fed regime of the upstream on-site treatment process (Figure 1). Each barrel (h = 1 m and V = 220 L) was bottom fed with an influent pipe passing down the center of the barrel, and overflowed to the next downstream barrel. The first two barrels were filled with 5-10 mm slag and the remaining barrels with 3-5 mm slag. 3-5 mm slag was used to increase the reactor longevity while 5-10 mm slag was used upstream to limit pressure build up by suspended solids. At the end of the five-barrel stream, the slag treated effluent overflowed into the concrete reactor inter-barrel space and was neutralized with $CO_2$-enriched air from the attached growth reactor that was coarse bubbled into the liquid. The $HRT_V$ for all 10 barrels was 15 h. The influent, barrel effluent and neutralization effluent were sampled periodically and analyzed for pH, alkalinity, TP, o-$PO_4$, calcium and fecal coliforms.

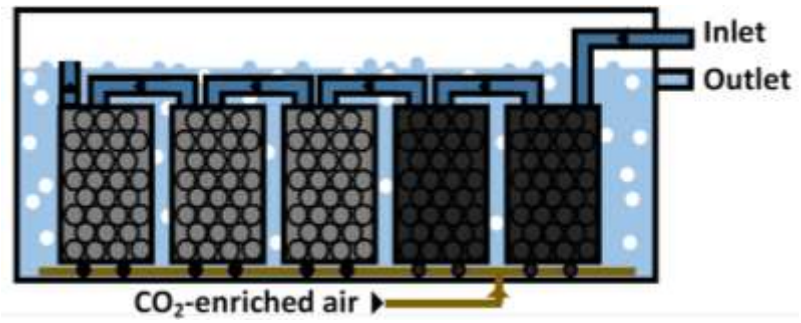


*Figure 1: Schematic of the barrel reactor test. Dark grey: 5-10 mm slag; pale grey: 3-5 mm slag (only one 5-barrel stream shown)*

## 2.6 Description of the P-Hydroslag model

The P-Hydroslag model is a mechanistic model that predicts o-$PO_4$ removal in steel slag filters. The main features of the model are presented in Table 4. Exhaustion functions coefficients were determined by a logistic function regression (equation 1). In equation 1, $CaO_{ltot}$ is the cumulative leached CaO from the slag (mol/g) while $P_1$ to $P_4$ are regression coefficients. $P_2$ is the saturation pH of fresh slag and $P_1$ is the minimum saturation pH reached after exhaustion. $P_3$ is the slope of the regression function and $P_4$ is the location of the inflexion point. The Gujer matrix of the model is presented in Claveau-Mallet et al. (2017).

*Table 4: Conceptual summary of the P-Hydroslag model (Claveau-Mallet et al., 2017)*

| Process | Description |
|---|---|
| Slag dissolution | Slag CaO dissolves following a first order equation with a saturation term (saturation pH). Slag stoichiometry is assumed to be 1CaO-0.3$CaCl_2$ following calcium calibration in batch tests. Slag aging is considered with experimentally measured exhaustion functions. Slag CaO leaching is limited by Fick's law of diffusion through a uniform thin film formed of precipitates. |
| P mineral precipitation | Precipitation of homogeneous hydroxyapatite, heterogeneous hydroxyapatite, monetite and calcite were considered with transformation of monetite into hydroxyapatite. Hydroxyapatite solubility is affected by particle size. Surface or precipitation reactions involving Fe/Al minerals at near-neutral pH were not considered. |

| | |
|---|---|
| Hydraulic flow | 1D flow in porous media with the advection-diffusion-reaction model. |

$$pH_{sat} = P_2 - \frac{P_2 - P_1}{\left(1 + e^{-P_3(CaOl_{TOT} - P_4)}\right)} \quad \text{eq. 1}$$

The specific surface of the slag was set at 2.76 x $10^6$, 1.84 x $10^6$ and 0.75 x $10^6$ $m^2/m^3$ for 2-3 mm, 3-5 mm and 5-10 mm slag, respectively. In the calibration work, the model was slightly modified compared to the previous model (Claveau-Mallet et al. 2017) to improve calibration quality. First, the slag stoichiometric composition was allowed to change according to slag exhaustion, instead of being constant. The slag formula was defined according to equation 2:

$$a_{CaO}CaO \cdot 2(1 - a_{CaO})NaOH \cdot a_{CaCl2}CaCl_2 \quad \text{eq. 2}$$

where $a_{CaO}$ and $a_{CaCl2}$ are stoichiometric coefficients. $a_{CaO}$ was always set between 0 and 1. As the slag stoichiometric coefficients were changing as a function of exhaustion, two-step exhaustion functions for slag stoichiometric coefficients were defined. Second, HAP heterogeneous precipitation was removed because HAP homogeneous precipitation yielded sufficiently good calibration results.

## 2.7 Numerical simulations

Column and barrel tests were simulated using PHREEQC and its IPHREEQC modules for interfacing with MATLAB (Charlton and Parkhurst 2011). The influent was simulated using the REACTION datablock and was put in equilibrium with calcite, monetite and hydroxyapatite using the EQUILIBRIUM_PHASES datablock. Detailed influent calibration results are provided in Appendix. The column and barrel tests were simulated using the TRANSPORT double porosity datablock with 20 numerical cells and a tolerance of $10^{-5}$. The hydraulic calibration was assumed from a previous column test with 5-10 mm slag (Claveau-Mallet et al. 2017). The hydraulic

parameters were effective porosity $n_e$ = 0.359, dispersivity D* = 5 cm and exchange factor between effective and immobile porosity $D_n = 5 \times 10^{-6}$ $s^{-1}$.

Barrel reactor scenarios were simulated by one five-barrel stream with an $HRT_V$ of 15 h. The first two barrels were filled with 5-10 mm slag and the remaining barrels with 3-5 mm slag. The replacement of the first barrel or the two first barrels was simulated by resetting to zero the kinetic reactions in numerical cells associated with replaced barrels. Barrels were replaced at a frequency of 0.5, 1, 1.5, 2, 2.5, 3, 3.5 or 4 years in accordance with a 6-month frequency maintenance required by the Quebec (Canada) regulation. Simulations were run for 14 years, which was arbitrarily defined as the maximum reactor longevity. Different simulations were run with fixed influent alkalinity between 50 and 210 mg $CaCO_3$/L.

### 2.7.1 Uncertainty associated with steel slag filter modeling and longevity criterion

Steel slag filter modeling is a challenge due to the high variability in the observed o-$PO_4$ concentration at effluent. Experimental o-$PO_4$-pH-Ca points generally follow the equilibrium state with hydroxyapatite predicted by the P-Hydroslag model, but there is noise in the relationship, as shown by Figure 2. In this Figure, experimental points from seven past studies conducted with EAF slag filters are compared to simulated curves in a realistic range for calcium (25 mg/L to 200 mg/L) and o-$PO_4$ (10 mg P/L). At pH between 8 and 9, the experimental variability can be fully explained by the model. At pH between 9 and 12, the experimental variability is greater than what can be predicted by the model. Such variability at high pH can be explained by a higher uncertainty in pH measurement above 10 or unstable calcium concentration in slag filters which could make equilibrium state unstable. A rapid drop in calcium concentration at effluent was reported in studies presented in Figure 2 and by Park et al. (2017).

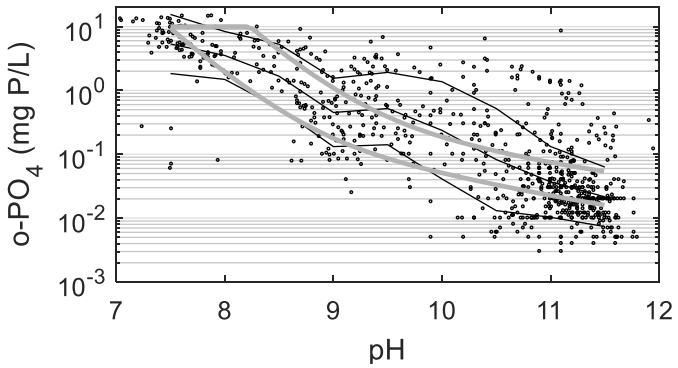


*Figure 2: Relationship between o-$PO_4$ and pH at effluent based on seven previous studies using EAF slag with synthetic, reconstituted or real wastewater (Abderraja Anjab 2009; Claveau-Mallet et al. 2012, 2013, 2015, 2017; Kõiv et al. 2016; Staingart 2012). Black lines indicate experimental mean and 1σ standard deviation curves. Gray lines indicate predicted o-$PO_4$ concentration at equilibrium with hydroxyapatite at Ca=25 mg/L (top curve) and Ca=200 mg/L (bottom curve)*

*In this study, the simulation quality criterion and longevity criterion were adapted to the modelling objective and considered the variability presented in Figure 2. Simulations were considered successful when they predicted accurate pH at all pH range, accurate o-$PO_4$ concentration in the pH range of 8 to 9.5 and approximate o-$PO_4$ concentration in the pH range of 9.5 to 12. This quality criterion was appropriate considering the modelling needs which were to predict the filter longevity, and not to predict accurate low o-$PO_4$ concentrations.*

The longevity (y) of the reactor was defined as the shortest duration determined according to three criteria: effluent pH reaching a low value of 10.0, effluent o-$PO_4$ reaching a high value of 0.4 mg P/L or reactor calcite accumulation reaching a high value of 0.2 mL CAL/L of void volume anywhere in the barrels. The pH criterion was set at a high value to ensure enough reactivity considering variability and uncertainty in the o-$PO_4$ – pH relationship (Figure 2). The o-$PO_4$ criterion was set below 1 mg/L to account for $X_P$ associated with o-$PO_4$. The clogging criterion was set according to the maximum reached in a previous study that was still flowing efficiently (Claveau-Mallet et al. 2017). The most constraining value of the three criteria was kept to assess the filter longevity. The pH criterion was found to be the limiting factor.

# 3 Results and Discussion

## 3.1 Effect of particle size on exhaustion functions

The exhaustion functions of the slag with different particle size are shown in Figure 3. The 5-10 mm data was determined in a previous study in which exhaustion functions were measured with the same synthetic water, same slag weight and same solution volume (Claveau-Mallet et al. 2017). In Figure 3, experimental data were represented by points while fitted exhaustion functions were represented by lines. The exhaustion functions parameters are provided in Table 5.

The saturation pH ($pH_{sat}$) was influenced by particle size (Figure 3A). The initial $pH_{sat}$ of slag with small particle size of 2-3 mm and 3-5 mm was 11.75 while it was 10.8 for 5-10 mm slag, and 8.75 for 16-23 mm slag. The $pH_{sat}$ exhaustion function of the 16-23 mm indicated that it is not suitable for steel slag filter applications because its saturation pH was too low. Slag of 2-3 mm and 3-5 mm had high initial $pH_{sat}$, which may improve mineral phase seeding, leading to more stable P retention compared to 5-10 mm slag. The first experimental point was not considered in the exhaustion function fitting to avoid a calibration artefact caused by the initial washing of the slag sample. Keeping the first data point in the exhaustion function had the effect to overestimate pH in the first days of operation and underestimate the longevity in the calibration work. A refined characterization of the initial slag washing would be possible by the addition of two or three acid baths with low acid concentration after the initial kinetic test. Exhaustion functions' uncertainty could be assessed by testing samples with different acid bath concentrations.

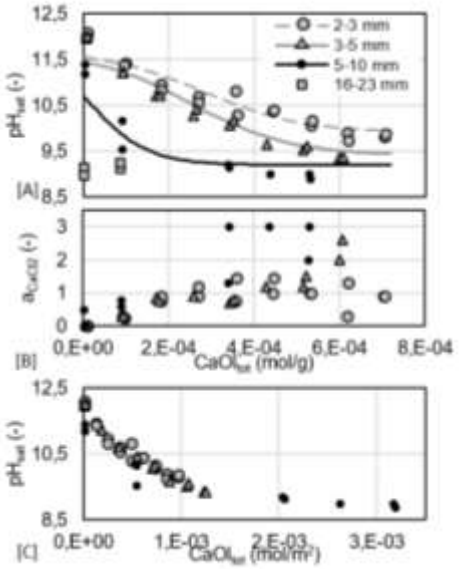


*Figure 3: Exhaustion functions of different slag particle size (points = experimental data; lines = fitted functions used in numerical simulations). Panel A: saturation pH. Panel B: calcium stoichiometry coefficient. Panel C: Same as panel A, but $CaOl_{tot}$ expressed by slag surface*

*Table 5: Exhaustion functions parameters*

| Slag particle | Regression coefficients | | | |
|---|---|---|---|---|
| | $P_1$ | $P_2$ | $P_3$ | $P_4$ |
| 2-3 mm | 9.9 | 11.7 | $8.50 \times 10^{3}$ | $2.80 \times 10^{-4}$ |
| 3-5 mm | 9.4 | 11.7 | $8.50 \times 10^{3}$ | $2.50 \times 10^{-4}$ |
| 5-10 mm | 9.2 | 12 | $1.45 \times 10^{4}$ | $1.00 \times 10^{-5}$ |

The slag CaO leaching capacity was approximately proportional to the specific surface (Figure 3C). In this figure, the X-axis leached CaO scale was converted from slag mass to slag surface. The 2-3 mm and 3-5 mm data were superimposed, indicating that the slag reactive CaO reservoir was proportional to its specific surface within this particle size range. The 5-10 mm data roughly followed the tendency of 2-3 mm and 3-5 mm data, with the pH being slightly

below. As the surface proportionality was validated, it would be possible to estimate exhaustion functions of slag media with various particle sizes from previous exhaustion functions. In future measurements of exhaustion functions, the authors recommend to express $CaOl_{tot}$ in mol/$m^2$ and to measure the specific surface of every tested slag samples, instead of assuming specific surface from a single analysis. This should reduce the variability caused by the heterogeneity of slag.

The slag stoichiometry was not constant following slag leaching (Figure 3B). In the initial model (Claveau-Mallet et al. 2017), the slag stoichiometry was constant and fixed at 1 CaO 0.3 $CaCl_2$. In the present work, step functions were defined according to Figure 3B (detailed in Table 6) to improve calcium calibration. These step functions are a simplification of the successive dissolution of different complex calcium oxides with decreasing solubility. Such a dissolution sequence was already observed by Kostura et al. (2005).

*Table 6: Slag stoichiometry used in simulations*

| Particle size | Step 1 | Step 2 |
|---|---|---|
| 2-3 mm | 0.7 CaO 0.6 NaOH before $3x10^{-4}$ mol/g | 1 CaO 0.75 $CaCl_2$ after $3x10^{-4}$ mol/g |
| 3-5 mm | 0.8 CaO 0.4 NaOH before $3x10^{-4}$ mol/g | 1 CaO 0.85 $CaCl_2$ after $3x10^{-4}$ mol/g |
| 5-10 mm | constant at 1.0 CaO 0.3 $CaCl_2$ | |

## 3.2 Model Calibration

The model calibration results are shown in Figure 4. The calibrated value of the crystal barrier diffusion coefficient was $D_{barr}$ = 2 x $10^{-13}$ $m^2$/s. The calibration of pH and calcium was good for the three particle sizes, showing that the model is suitable for various particle sizes with a single calibration. The alkalinity calibration was acceptable, with simulated curves slightly below

experimental data. The model predicted accurate o-$PO_4$ concentration of 0.8-1 mg P/L when the pH was between 9 and 10 (column 3).

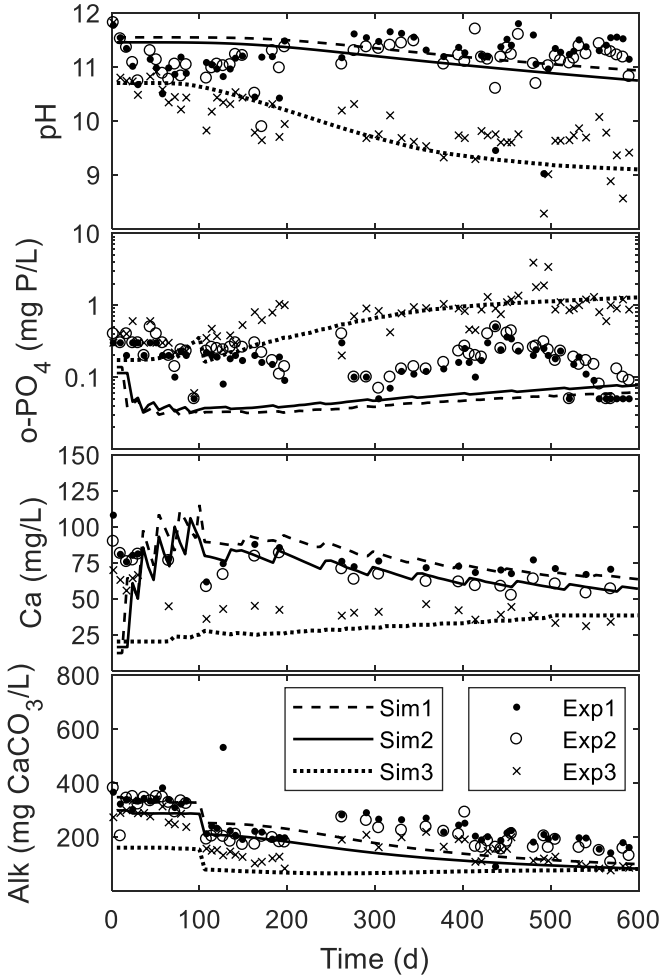


*Figure 4: Calibration of the P-Hydroslag model using three column tests with different particle size. Exp1 and Sim1: 2-3 mm, Exp2 and Sim2: 3-5 mm, Exp3 and Sim3: 5-10 mm*

The o-$PO_4$ experimental data of columns 1 and 2 did not agree with the equilibrium state predicted by the model. The model predicted an effluent concentration between 0.04 and 0.05 mg P/L, while experimental data ranged between 0.04 and 0.40 mg P/L. The experimental o-$PO_4$ data of columns 1 and 2 were superimposed and they followed three general trends: a slow

decrease from 0 to 250 d, followed by a slow rise from 250 to 450 d and finally a slow decrease from 450 to 600 d. The same trends were roughly observed in the influent o-$PO_4$ concentration, which suggests that o-$PO_4$ precipitation kinetic rates may be more complex. This limitation is acceptable considering the simulation quality criterion defined previously.

## 3.3 Model Validation

The model validation results using the barrel reactor test data are shown in Figure 5. pH was considered as the most important parameter for model validation, because it reflects the slag reactivity and thus, the filter longevity. The pH drop had not yet been seen in experimental data, except for barrel 1. The simulated pH curve of barrel 1 followed experimental data, while it dropped too early for barrels 2 to 5. The slight underestimation of pH remains appropriate for design purpose, meaning that the model yields conservative scenarios of longevity prediction. Note that the low pH observed in all barrels at 200 d was related to an episodic event of high strength in the influent.

The discrepancy between simulated and experimental pH may be explained, notably, by the slag sieving protocol. Simulations were realized using exhaustion functions that were measured on a small slag sample rigorously sieved to the required particle size prior to the test. For the barrels test, slag was sieved at the slag mill at industrial scale, transported by trucks and filled into the barrels on site. This slag preparation method resulted in some slag particle breaking during transportation, as confirmed by small slag grains visible during barrel filling. Thus, the 5-10 mm barrels contained slag smaller than 5 mm in an unknown proportion, which increased its reactivity. It resulted in experimental pH of barrels 1 and 2 being higher than what predicted by the 5-10 mm exhaustion function. The increase of the 5-10 mm barrels reactivity was considered in the validation by using a slightly increased exhaustion function for 5-10 mm slag (P1=9.35,

P2=11.3, P3=1.1 x $10^{4}$, P4=2 x $10^{-4}$), but the barrel 2 pH was still underestimated (Figure 5). A similar issue was observed in a previous slag column study in which the measured exhaustion function was too low to reproduce correctly column pH data (Claveau-Mallet et al. 2017). In this former study, the column was filled with 5-10 mm that was sieved at the slag mill. The column tests of the present study were hand-sieved onsite just before filling, which limited particle breaking. It resulted in pH effluent data that agreed with the 5-10 mm simulation (Figure 4). In conclusion, the type of slag sieving and transportation affects the slag particle size, thus affecting its reactivity. The authors recommend to study more in depth this phenomenon in a quantitative manner, to reduce the simulation uncertainty.

It was not possible to validate the model using o-$PO_4$ data because the filter had not yet reached its o-$PO_4$ breakthrough. The model underestimated o-$PO_4$ at low o-$PO_4$ concentrations, as observed in the calibration step. In the first 150 days, the simulated o-$PO_4$ concentration was 0.03 mg P/L in barrels 2 to 5, while experimental data ranged between 0.1 and 0.5 mg P/L. The simulated and experimental calcium data were in the same order of magnitude. The simulated alkalinity was slightly lower than the experimental data. Note that the alkalinity peak observed in experimental data between 150 and 200 d was caused by an influent peak in alkalinity. Further studies with long-term operation of barrel reactors should be conducted to reinforce the model robustness.

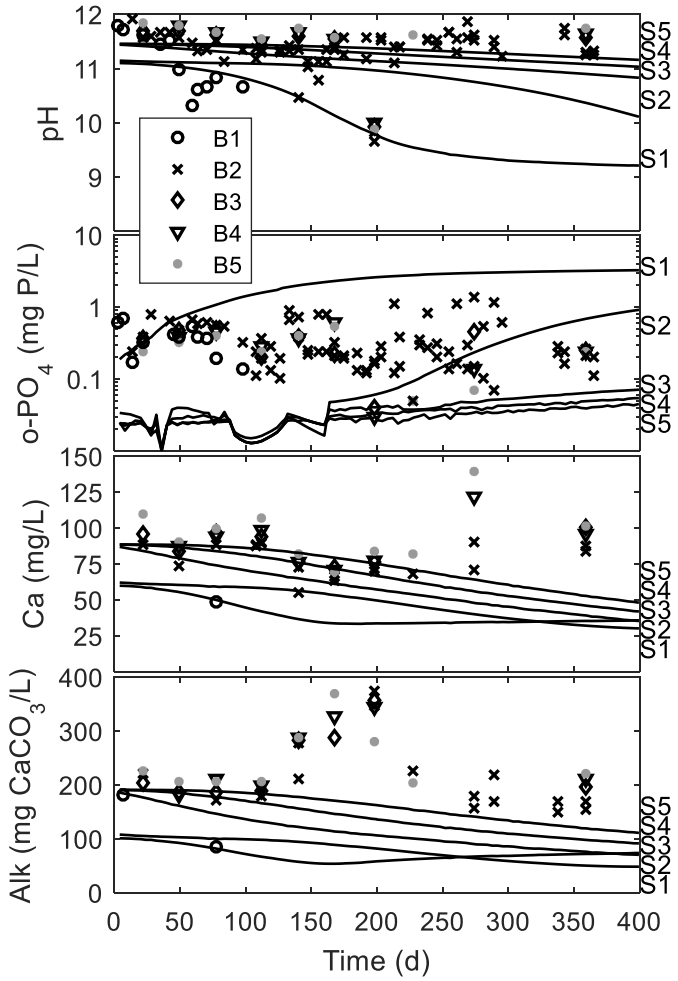


*Figure 5: Validation of the P-Hydroslag model using a barrel reactor test. Points: experimental data, labelled with B as indicated in the legend. Lines: simulated data of barrels 1 to 5, labelled with S on the right Y axis.*

## 3.4 Particulate phosphorus in steel slag filters

The particulate phosphorus concentration ($X_P$) at the influent and effluent of column tests is shown in Figure 6. $X_P$ was defined as total phosphorus minus o-$PO_4$. All slag columns removed about 50% of $X_P$ at any influent concentration between 0 and 2.5 mg P/L. 2-3 mm slag (column 1) and 3-5 mm slag (column 2) had a similar removal efficiency, while 5-10 mm slag (column 3) had slightly poorer removal performance due to its coarser size. Similar removal efficiency was

observed by Kõiv et al. (2016), who fed 5-10 mm steel slag columns with a fish farm effluent. Under low-strength conditions ($X_P$ = 0.25 mg P/L at influent), these authors observed a mean value of $X_P$ = 0.1 mg P/L in the effluent. The $X_P$ removal efficiency was approximately the same under high-strength conditions ($X_P$ = 15 and 5 mg P/L in the influent and effluent, respectively).

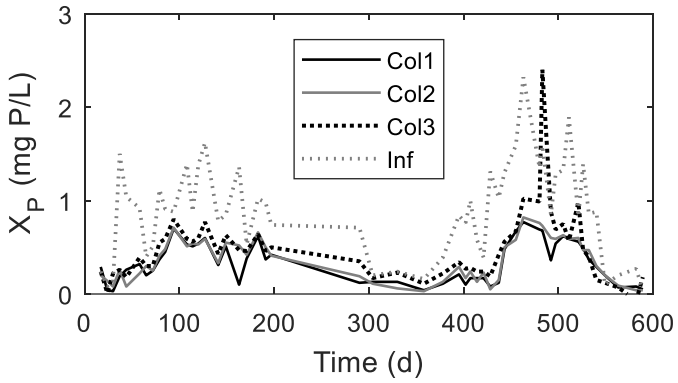


*Figure 6: Evolution of particulate phosphorus ($X_P$) in the column test (experimental data)*

The type and efficiency of the secondary treatment process had an influence on its $X_P$ concentration in the effluent, thus influencing the $X_P$ concentration at the effluent of the steel slag filter. This effect was observed by comparing the column and barrel reactor tests, which had different upstream secondary treatment processes. The column test influent (from aerated lagoons) had a mean total suspended solid (TSS) concentration of 19 mg/L associated with $X_P$ between 0.2 and 2 mg P/L (Figure 6). The barrel reactor test influent (from attached growth aerated reactor) had a TSS concentration of 15 mg/L with an $X_P$ concentration of 0.4 mg P/L, which is lower than the concentrations observed coming out of the aerated lagoons. Consequently, the $X_P$ concentration in the barrel reactor test effluent was very low (mean of 0.06 mg P/L). The mean o-$PO_4$/TP ratio observed in the effluent of the barrel reactor test was 0.93. These results indicate that, as expected, there is a relationship between TSS and $X_P$ in the upstream process that must be considered in the design of steel slag filters. An efficient

secondary treatment is needed to ensure efficient P removal in the steel slag filters, because of a limited $X_P$ filtration efficiency; and limit pressure build up in the filter. In Quebec (Canada) regulations, such efficient secondary treatment is called advanced secondary treatment, which involves a requirement of TSS = 15 mg/L in the effluent (MDDELCC 2017). For design purposes, it is recommended to consider an effluent o-$PO_4$/TP ratio of 0.9. Consequently, the TP target of 1 mg P/L corresponds to a o-$PO_4$ longevity target of 0.9 mg P/L in simulations.

Removal mechanisms of $X_P$ in steel slag filters are chemisorption and filtration. Chemisorption means that newly formed calcium phosphate precipitates are incorporated in a fixed crystal matrix by crystal growth or sorption. The hypothesis that newly formed calcium phosphate precipitates are stable and not leached is reasonable considering the low turbulence in steel slag filters and high organization of crystals (Claveau-Mallet et al. 2012). Filtration is the main mechanism that affects the removal of influent $X_P$. Results of this study indicated a roughly constant removal efficiency independently of influent concentration, which is in agreement with the first-order kinetic of filtration accepted in the literature (Tufenkji and Elimelech 2004). The small influence of slag particle size on filtration efficiency, however, does not agree with common filtration theory. This result may be attributed to the large particle size of the slag filters, compared to drinking filtration processes in which particle size is typically below 1 mm. Filtration models (Tufenkji and Elimelech 2004) may not be directly applicable to gravel-sized filters. The authors recommend to study the fractionation of $X_P$ in steel slag filters in order to validate the role of filtration and chemisorption. Organic and inorganic $X_P$ as well as colloidal phosphorus may have different fates in steel slag filters.

## 3.5 Slag barrel replacement management

The calibrated model was used to simulate long-term operation of a slag barrel reactor as shown in Figure 1. Different barrel replacement strategies were tested to optimise the filter longevity and barrel needs. An example of a slag filter simulation with replacement of the two first barrels is shown in Figure 7A and B.

The objective of partial barrel replacements was to increase the longevity of the whole system and ease maintenance logistics by replacing only the first two barrels once they become exhausted by clogging. In steel slag filters, chemical clogging is caused mainly by precipitation of calcite. It is possible to predict calcite accumulation in each barrel using simulations, as shown in Figure 7B. In that specific simulation, calcite accumulation was located mainly in the first two barrels, which are replaced every two years, and to a less extent in barrel 3. Calcite accumulation in barrels 3 to 5 was delayed by the frequent replacement of barrels 1 and 2. Calcite formed in barrel 5 after 5 years of operation only. In low-alkalinity influent, it was possible to strongly limit calcite accumulation. For example, an influent with 50 mg $CaCO_3$/L of alkalinity and replacement of barrels 1 and 2 every 2 years resulted in calcite accumulation of 0.01 mL calcite / mL water in barrel 5 after 14 years. Without partial barrel replacements, the system longevity was between 7 years (influent alkalinity of 50 mg $CaCO_3$/L) and 2 years (influent alkalinity of 210 mg $CaCO_3$/L), as indicated in Figure 7C. The simulations presented in Figure 7C are compatible with the 6-month maintenance regulation applicable in Quebec, Canada. The simulation results can be included in a technico-economical analysis that considers the system longevity and associated costs for maintenance (cost of barrels, cost of partial barrel replacement mobilization, cost of whole system replacement mobilization). It is worth to note that partial replacements slightly increased the global barrel needs of the system. As an example, the total number of barrels needed for a 100 mg $CaCO_3$/L alkalinity influent was 2.22

barrels/year without partial replacements, and 2.54 barrels/year if the first two barrels were replaced every three years.

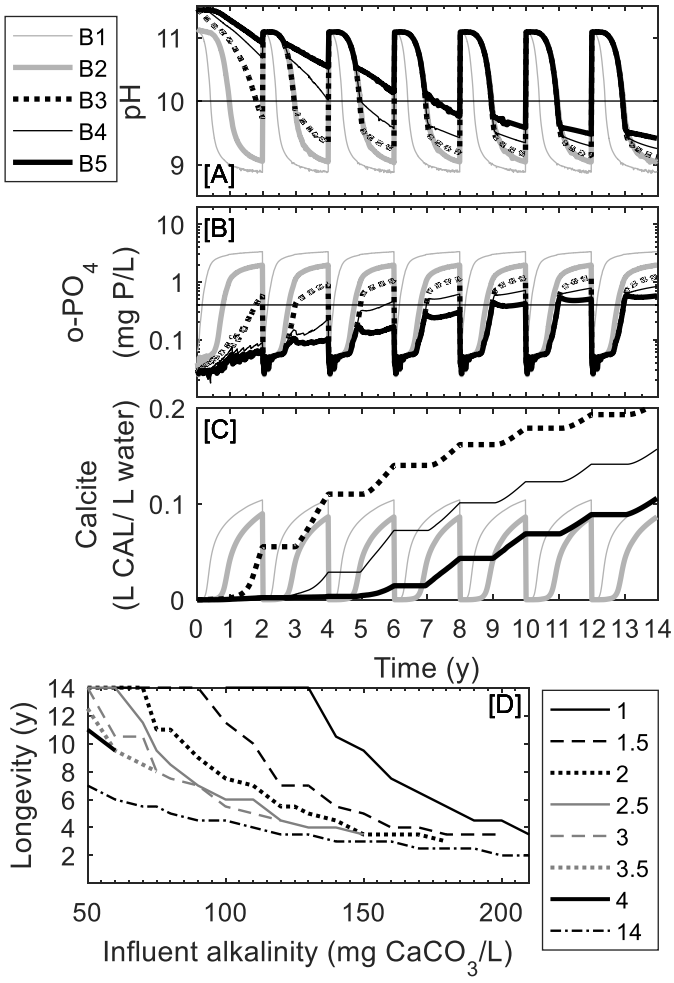


*Figure 7: Optimization of slag filter replacement using modelling. Panels A, B and C: 14-year simulation of a steel slag barrel reactor with influent alkalinity = 100 mg $CaCO_3$/L and replacement of barrels 1 and 2 every 2 years. Panel A: pH at effluent of barrels 1 to 5 (longevity criterion at pH = 10 is indicated with a horizontal line). Panel B: o-$PO_4$ at effluent of barrels 1 to 5 (longevity criterion at o-$PO_4$ = 0.4 mg P/L is indicated with a horizontal line). Panel C: Calcite accumulation in barrels 1 to 5. Panel D: Effect of maintenance frequency and influent alkalinity*

*on the slag filter reactor longevity. Replacement frequency of barrels 1 and 2 are indicated in the legend (years)*

The longevity criterion for calcite accumulation was defined because head loss buildup in the slag filters must be limited to avoid overflow in the upstream process. Two types of clogging occur in steel slag filters: chemical (calcite and calcium phosphate accumulation, cementation) and physical (accumulation of suspended solids from the influent). The P-Hydroslag model used in this project could predict chemical clogging with a quantitative evaluation of calcite accumulation, but it could not associate it to a pressure build-up. Physical clogging was not considered in this model. The next step for model development would be to predict head loss evolution in the filter considering both chemical and physical clogging. Long-term hydraulic characteristics of the barrel reactor should be evaluated with tracer tests conducted several times during the filter lifetime (ex. reduction in void volume, development of short-circuiting). Other full-scale applications of steel slag filters in horizontal flow beds have shown an evolution of tracer test response over 29 weeks of operation (Barca et al. 2018), which show that initial hydraulic properties cannot be assumed for the whole lifecycle of the filter.

Simulations with replacement of the first barrel only indicated that this option was not satisfactory due to excessive calcite precipitation in the second barrel. This behavior is related to slag dissolution kinetic. In the first barrel, there is enough reaction time to increase the influent pH, but not enough to reach a pH that favors calcite precipitation. As a result, for a fixed influent composition, changing the first two barrels every two years resulted in improved longevity compared to replacement of the first barrel every year.

In future research, the barrel reactor geometry will be optimized to limit long term pressure build-up. Factors such as water distribution in the barrels, slag particle size sequence and backwash maintenance will be considered.

## 3.6 Fate of alkalinity in decentralized wastewater treatment

Alkalinity is a major factor that influences the steel slag filter longevity because of chemical clogging, as shown in Figure 7C. It is therefore important to understand the origin and fate of alkalinity in decentralized wastewater treatment. Assuming that the steel slag filter is a tertiary treatment process, it is useful to study the fate of alkalinity in all steps prior to tertiary treatment: drinking water source, primary treatment and secondary treatment.

In many decentralized applications, the source of drinking water is groundwater from individual wells. In Quebec (Canada), 20% of the population has groundwater as water supply (MDDELCC 2018). The alkalinity of natural groundwater is related to the type of aquifer. A systematic study of groundwater quality in the Abitibi region (Quebec, Canada) showed that sediment-based aquifers have lower alkalinity than fractured-rock aquifers (Cloutier et al. 2013). These authors reported 125 mg/L of $HCO_3$ in granular aquifers and 200-260 mg/L of $HCO_3$ in rock aquifers. They also observed higher mineralization in captive aquifers compared to free surface aquifers. Lower alkalinity may be observed in wells located in alluvial sediments close to lakes or rivers (Bourg and Bertin 1993).

In secondary treatment, an important process that affects alkalinity is nitrification. Nitrification is commonly seen as a process that has stoichiometric needs in alkalinity (Metcalf and Eddy - AECOM 2014). For steel slag filter design, one needs to describe nitrification in a more rigorous way. Complete nitrification transforms ammonium into nitrate following equation 3, reducing pH due to $H^+$ production. The pH reduction causes a shift of the carbonate equilibrium to the

$CO_2$ size, which lead to $CO_2$ stripping if good mixing conditions are present. Therefore, nitrification reduces alkalinity by both pH reduction and $CO_2$ stripping.

$$NH_4^+ + 2O_2 \rightarrow NO_3^- + 2H^+ + H_2O \qquad \text{eq. 3}$$

In steel slag filter applications, it is useful to reduce the inorganic carbon concentration of the influent by $CO_2$ stripping to reduce the filter clogging by $CaCO_3$. In the proposed process configuration, nitrification is achieved in a confined biological process with an air reservoir with $CO_2$-enriched air which is used for neutralization of the steel slag filter effluent (Bove et al. 2018). As $CO_2$ stripping follows Henry's law, the inorganic carbon concentration reduction induced by nitrification is influenced by the $CO_2$ enriched-air concentration. A $CO_2$ enriched-air concentration of 1000 to 5000 ppm is expected in a confined biological process with steel slag filter neutralization (Bove et al. 2018). The effect of nitrification on stripped $CO_2$ under different conditions is shown in Figure 8. $CO_2$ stripping was favored at low $CO_2$ concentration in the enriched air. $CO_2$ stripping was maximized at an influent alkalinity of 60-80 mg $CaCO_3$/L.

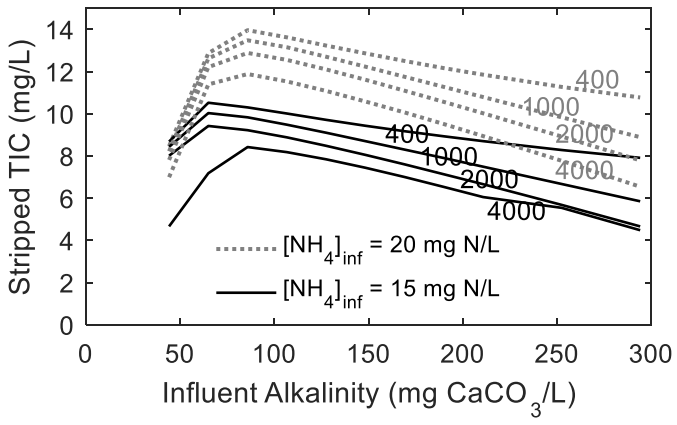


*Figure 8: Influence of nitrification on TIC removal in the biological process by $CO_2$ stripping. $CO_2$ concentration in the biological process confined air is indicated next to lines (ppm)*

The best way to increase the steel slag filter longevity is to reduce its influent carboneous alkalinity. The implementation of a secondary treatment with nitrification prior of the steel slag would reduce the alkalinity. In cold climates, nitrification may not be active. The chemical dosage of $NaHCO_3$ in the secondary treatment should be avoided. If it is needed for nitrification, it should be strictly designed to avoid excess $NaHCO_3$. In common small decentralized applications (influent flowrate below 3240 L/d), however, no $NaHCO_3$ is added. The dosage of iron coagulant and settling prior to the steel slag filter may promote alkalinity reduction by co-precipitation of calcite (Metcalf and Eddy - AECOM 2014). This option is possible in WRRFs, but is not common in small decentralized applications. $CO_2$ enrichment in the secondary treatment head air must be limited to ease $CO_2$ stripping in the nitrification stage. The use of the enriched air for neutralization is a useful way to reduce its $CO_2$ concentration. Another approach would be to ventilate the reactor headspace. Finally, steel slag filter designers may recommend this process mainly for low alkalinity drinking water sources. This recommendation may be contradictory with water quality requirements, as groundwater from confined aquifers is safer than free-surface groundwater regarding microbial contamination.

# 4 Conclusion

The objective of this project was to develop a novel phosphorus removal system using steel slag filters applicable in decentralized applications and propose design criteria about maintenance needs. The novel system was made of two parallel streams of five replaceable steel slag barrels followed by neutralization with $CO_2$-enriched air in the inter-barrel space.

Exhaustion functions were measured on four slag particle sizes. The initial saturation pH was 11.75 for 2-3 mm and 3-5 mm slag while it was 10.8 for 5-10 mm slag, and 8.75 for 16-23 mm slag. Different saturation pH suggested that the mineralogical composition at the slag surface is influenced by particle size. The slag CaO leaching capacity was approximately proportional to the specific surface, which means that it would be possible to estimate exhaustion functions of slag media with various particle sizes from previous exhaustion functions. In future measurements of exhaustion functions, the authors recommend to express the slag CaO leaching by slag surface instead of slag mass.

The P-Hydroslag model was calibrated using three steel slag filters column tests with particle size of 2-3 mm, 3-5 mm and 5-10 mm and fed with the effluent of an aerated lagoon. The calibration of pH and calcium was good for the three particle sizes. The addition of step functions in the slag stoichiometry improved the calcium calibration. The o-$PO_4$ calibration at the beginning of the filter operation underestimated experimental data, but was accurate to predict the pH-drop region, which was acceptable considering the modelling objective of longevity prediction.

The calibrated model was validated using a dataset from a full-scale 5-barrel reactor fed with the effluent of an attached growth aerated biological reactor. The simulated pH slightly underestimated experimental data. This slight underestimation of pH remains appropriate for

design purpose, meaning that the model yields conservative scenarios of longevity prediction. Thus, the P-Hydroslag model was shown to be effective for reactor design for real wastewater conditions. The slag transportation and filling protocol resulted in particle breakage, which increased the barrel reactivity.

The three steel slag filter columns removed roughly 50% of particulate phosphorus. The type and efficiency of the upstream secondary treatment process had an influence on its particulate phosphorus concentration at effluent, thus influencing the particulate phosphorus concentration at the effluent of the steel slag filter. Upstream processes with efficient TSS removal (lower than 15 mg/L) are recommended to ensure low total phosphorus at the effluent of the steel slag filter.

The calibrated model was used to simulate a full-scale long-term operation of a slag barrel reactor with two parallel streams of five replaceable steel slag barrels, with total hydraulic retention time of voids of 15 h. Three longevity criteria were defined: reaching an effluent pH of 10.0, reaching an effluent o-$PO_4$ concentration of 0.4 mg P/L and reaching a clogging value of 0.2 mL calcite /mL of water in any barrel. The system longevity was influenced by the influent alkalinity. It was estimated to be 7 years with an influent of 50 mg $CaCO_3$/L and 2 years with influent of 210 mg $CaCO_3$/L. In typical decentralized applications with groundwater drinking water source, the influent alkalinity is influenced by the type of aquifer and presence of nitrification in the upstream biological process. Scenarios with partial barrel replacement increased the system longevity of up to 14 years while slightly increasing the number of barrels needed. The next step for model development would be to predict head loss evolution in the filter considering both chemical and physical clogging.

# 5 Acknowledgements

This work was funded by the Natural Sciences and Engineering Research Council of Canada (grant 476673-14), the MITACS Accelerate program (grant IT09967), Bionest, ArcelorMittal, Harsco Minerals, AgroÉnergie, GHD consulting, the RAQ (*Ressources aquatiques Québec*) and NORDIKEau. The authors thank Denis Bouchard, Jérôme Leroy and Manon Leduc from Polytechnique Montreal for analytical determinations. The authors also thank Serge Baillargeon, Marc Boissonnault, Wiliam Narbey, Philie Dallaire, Félix Lida and Céline Khuu from Bionest.

# 6 References

Abderraja Anjab, Z. (2009). *Development of a steel slag bed for phosphorus removal from fishfarm wastewater (In French).* M.A.Sc. thesis, Polytechnique Montreal, Canada.

Barca, C., N. Roche, S. Troesch, Y. Andrès and F. Chazarenc. 2018. Modelling hydrodynamics of horizontal flow steel slag filters designed to upgrade phosphorus removal in small wastewater treatment plants. Journal of Environmental Management 206, 349-356.

Bionest Wastewater Treatment Solutions. 2018. Our products - Aerated lagoons KAMAK. Retrieved from http://www.bionest-tech.com/QC-en/product/20-406/.html. Accessed on January 24th 2018.

Blanco, I., P. Molle, L. Sáenz de Miera and G. Ansola. 2016. Basic Oxygen Furnace steel slag aggregates for phosphorus treatment. Evaluation of its potential use as a substrate in constructed wetlands. Water Research 89, 355-365.

Bourg, A. C. and C. Bertin. 1993. Biogeochemical Processes during the Infiltration of River Water Into an Alluvial Aquifer. Environmental Science and Technology 27, 661-666.

Boutet, É., S. Baillargeon, F. Allaire, F. Lida, D. Claveau-Mallet and Y. Comeau. 2017. Apparatus and method for wastewater treatment, US Provisional Patent Application No. 62/450,210, filed January 25, 2017.

Bove, P., D. Claveau-Mallet, É. Boutet, F. Lida and Y. Comeau. 2018. Design and modelling of a steel slag filter effluent neutralization process with passive CO2-enriched air. Water Research 129, 11-19.

Bunce, J. T., E. Ndam, I. D. Ofiteru, A. Moore and D. W. Graham. 2018. A Review of Phosphorus Removal Technologies and Their Applicability to Small-Scale Domestic Wastewater Treatment Systems. Frontiers in Environmental Science 6(8), 1-15.

Charlton, S. R. and D. L. Parkhurst. 2011. Modules based on the geochemical model PHREEQC for use in scripting and programming languages. Computers & Geosciences 37(10), 1653-1663.

Claveau-Mallet, D., B. Courcelles, P. Pasquier and Y. Comeau. 2017. Numerical Simulations with the P-Hydroslag Model for Prediction of Phosphorus Removal by Steel Slag Filters. Water Research 126, 421-432.

Claveau-Mallet, D., F. Lida and Y. Comeau. 2015. Improving phosphorus removal of conventional septic tanks by a recirculating steel slag filter. Water Quality Research Journal of Canada 50(3), 211-218.

Claveau-Mallet, D., S. Wallace and Y. Comeau. 2012. Model of phosphorus precipitation and crystal formation in electric arc furnace steel slag filters. Environmental Science and Technology 46(3), 1465-1470.

Claveau-Mallet, D., S. Wallace and Y. Comeau. 2013. Removal of phosphorus, fluoride and metals from a gypsum mining leachate using steel slag filters. Water Research 47(4), 1512-1520.

Cloutier, V., D. Blanchette, P.-L. Dallaire, S. Nadeau, E. Rosa and M. Roy. 2013. Project of knowledge acquisition on groundwater in Abitibi-Témiscamingue (In French). Report presented to the *Ministère du développement durable, de l'environnement, de la faune et des parcs*, program of knowledge acquisition on Quebec groundwater. Quebec University in Abitibi-Témiscamingue, Report number P001. Retrieved from http://www.mddelcc.gouv.qc.ca/_PACES/rapports-projets/Abitibi/ABI-scientif-UQAT-201309.pdf.

Hussain, S. I., D. W. Blowes, C. J. Ptacek, J. H. Jamieson-Hanes, B. Wootton, G. Balch and J. Higgins. 2015. Mechanisms of phosphorus removal in a pilot-scale constructed wetland/BOF slag wastewater treatment system. Environmental Engineering Science 32(4), 340-352.

Kõiv, M., K. Mahadeo, S. Brient, D. Claveau-Mallet and Y. Comeau. 2016. Treatment of fish farm sludge supernatant by aerated filter beds and steel slag filters - effect of organic loading rate. Ecological Engineering 94, 190-199.

Kostura, B., H. Kulveitová and J. Leško. 2005. Blast furnace slags as sorbents of phosphate from water solutions. Water Research 39(9), 1795-1802.

MDDELCC. 2018. Groundwater (In French). *Ministère du Développement durable, de l'Environnement et de la Lutte contre les changements climatiques*, Government of Quebec. Retrieved from http://www.mddelcc.gouv.qc.ca/eau/souterraines/index.htm#puits, Accessed on March 27th 2018.

MDDELCC. 2017. Technical Guide – Wastewater Treatment of Remote Dwellings (In French). *Ministère du Développement durable, de l'Environnement et de la Lutte contre les changements climatiques*, Government of Quebec. Retrieved from http://www.mddelcc.gouv.qc.ca/eau/eaux-usees/residences_isolees/guide_interpretation/index.htm

Metcalf & Eddy - AECOM, G. Tchobanoglous, H. D. Stensel, R. Tsuchihashi and F. Burton. 2014. Wastewater engineering: treatment and resource recovery. McGraw-Hill, New York.

Park, T., V. Ampunan, S. Maeng and E. Chung. 2017. Application of steel slag coated with sodium hydroxide to enhance precipitation-coagulation for phosphorus removal. Chemosphere 167, 91-97.

Penn, C., J. Bowen, J. McGrath, R. Nairn, G. Fox, G. Brown, S. Wilson and C. Gill. 2016. Evaluation of a universal flow-through model for predicting and designing phosphorus removal structures. Chemosphere 151, 345-355.

Postila, H., S. M. Karjalainen and B. Kløve. 2017. Can limestone, steel slag or man-made sorption materials be used to enhance phosphate-phosphorus retention in treatment wetland for peat extraction runoff with low phosphorus concentration? Ecological Engineering 98, 403-409.

Staingart, A. (2012). Phosphorus removal fromp septic tank effluents by coarse steel slag (In French). M.Eng. thesis, Polytechnique Montreal, Canada.

Stumm, W. and J. J. Morgan. 1996. Aquatic Chemistry: Chemical Equilibria and Rates in Natural Waters. 3rd edition, John Wiley & Sons, New York.

Tufenkji, N. and M. Elimelech. 2004. Correlation equation for predicting single-collector efficiency in physicochemical filtration in saturated porous media. Environmental Science and Technology 38, 529-536.

Vohla, C., M. Kõiv, H. J. Bavor, F. Chazarenc and Ü. Mander. 2011. Filter materials for phosphorus removal from wastewater in treatment wetlands-A review. Ecological Engineering 37(1), 70-89.

Zuo, M., G. Renman, J. P. Gustafsson and W. Klysubun. 2017. Dual slag filters for enhanced phosphorus removal from domestic waste water: performance and mechanisms. Environmental Science and Pollution Research, 1-10.

# 6 Appendix

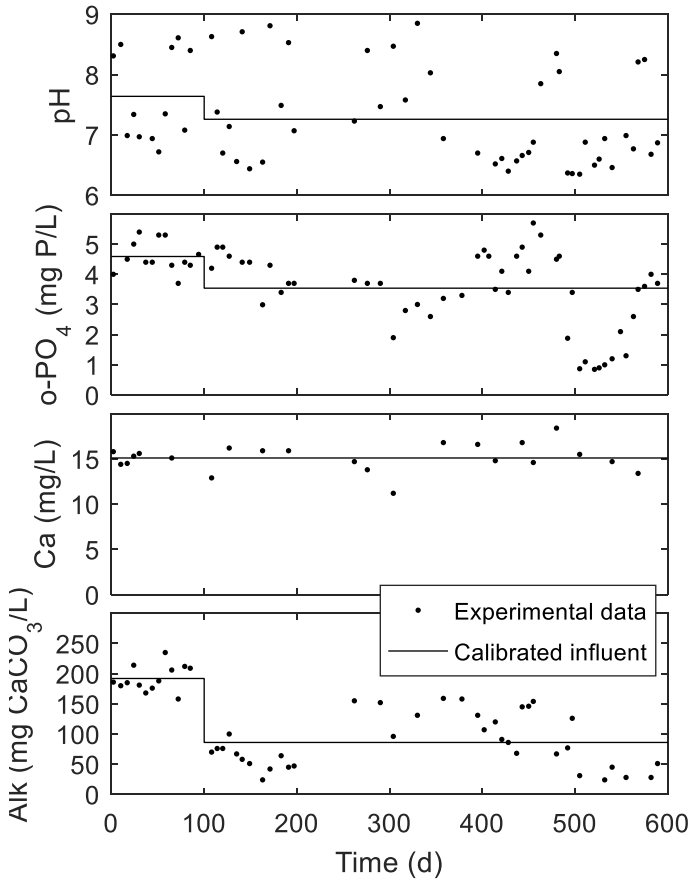


*Figure 9: Effluent composition monitoring at the the Grandes-Piles WRRF (experimental data) and influent calibration of the column test simulation*

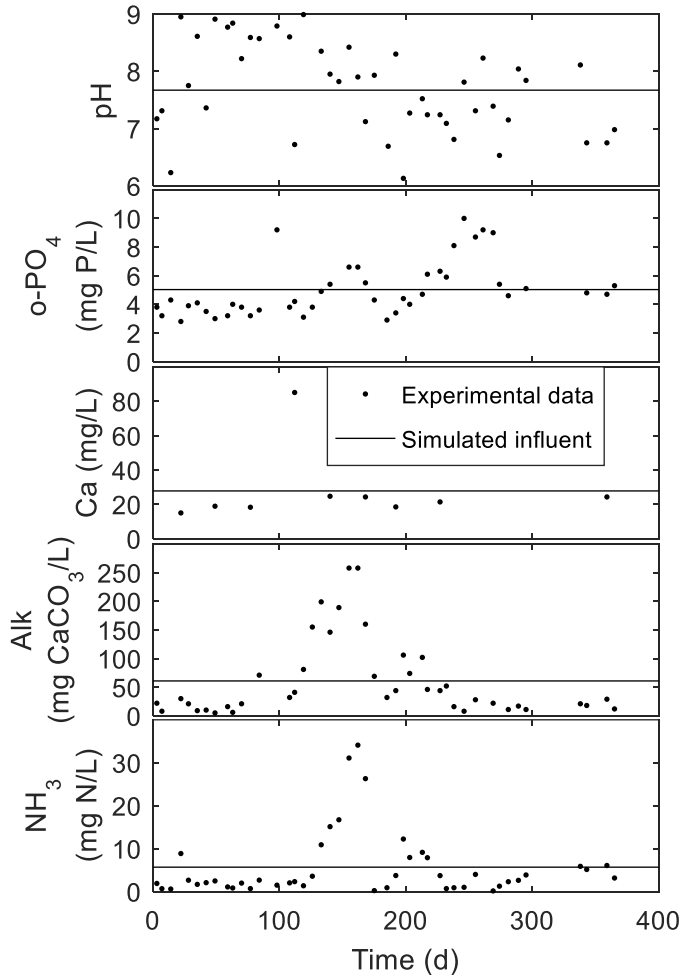


*Figure 10: Influent composition monitoring of the barrel reactor test (experimental data) and influent calibration of the barrel test simulation*